International Journal of Innovative Computing, Information and Control
Volume **10**, Number **5**, October **2014**

ICIC International ©2014 ISSN 1349-4198
pp. 1727–1745

VALIDITY OF PRODUCTION FLOW DETERMINED BY THE PHASE DIFFERENCE IN THE GRADIENT SYSTEM OF AN AUTONOMOUS DECENTRALIZED SYSTEM

Kenji Shirai[1] and Yoshinori Amano[2]

[1]Faculty of Information Culture
Niigata University of International and Information Studies
3-1-1, Mizukino, Nishi-ku, Niigata 950-2292, Japan
shirai@nuis.ac.jp

[2]Kyohnan Elecs Co., LTD.
8-48-2, Fukakusanishiura-cho, Fushimi-ku, Kyoto 612-0029, Japan
y_amano@kyohnan-elecs.co.jp

Received November 2013; revised March 2014

Abstract. *In this study, we verify that the production flow process is reasonable by determining the phase difference in the gradient system of an autonomous decentralized system. We set a target throughput for each work process, and workers attempt to maintain this target throughput. The working method is reasonable for the production process. To analyze the production flow process, we use the phase difference in the gradient system of an autonomous distributed system. Specifically, it is possible to synchronize processes by maintaining a constant phase difference in the gradient system of an autonomous decentralized system. By achieving synchronization between processes, the entire process plays a role in maintaining the target throughput.*
Keywords: Production flow process, Gradient system, Synchronous process, Autonomous decentralized system, Potential

1. **Introduction.** Several studies have addressed the problem of productivity improvement in industrial production processes [1, 2]. Moreover, various theories have been applied to improve and reform production processes and increase productivity. In [3], an analysis that uses the queuing model and applies a log-normal distribution to model a system in the steel industry is described.

Several studies have reported approaches to shorten lead times [4, 5]. From the time of product ordering, the lead time is dependent on the work required to prepare the system for production.

We have reported that an analysis of the rate-of-return deviation for a certain equipment manufacturer over the past ten years displays "power-law distribution characteristics". Because the power-law distribution reveals the existence of a phase transition phenomenon, we expect that the rate-of-return deviation and the production system are correlated in a manner that is mediated by the power-law distribution [6]. By performing a data analysis, the relation between the rate-of-return deviation and production throughput has been clarified to some extent. The "fluctuation model of rate-of-return deviation" is self-similar and shows a fractal nature [7, 20]. Also, this power-law distribution characteristic has a "fluctuating" nature during phase transition. For example, occurrence of fluctuation is found at where the phase transition occurs at the point. Then, we have reported on the self-similarity of these fluctuations and noted the f^{-1} and f^{-2} fluctuations [8]. We have also verified self-similarity in the system through experiments on the supply

chain system, and have used the supply chain system to produce control equipment. In total, nine workers were involved, and the production process was composed of six stages. To compare the forms of production, we roughly conducted four patterns of asynchronous and synchronous methods. In this report, we propose that it is possible to increase manufacturing profits by adopting a management strategy that purposefully leads to a state of excessive production or excessive order entries. This management strategy is ideal on the basis of analysis of the cost rate of the production process.

Although the traditional approach to avoiding bottlenecks in production processes is to use the theory of constraints [9], we have reported that the synchronization method is superior for shortening throughput in production processes. This method requires synchronization between processes [10].

In our previous study [11], we constructed a state in which the production density of each process corresponded to the physical propagation of heat [20]. Using this approach, we showed that a diffusion equation dominates the production process. In other words, when minimizing the potential of the production field (stochastic field), the equation, which is defined by the production density function $S_i(x,t)$ and boundary conditions, is described by the use of diffusion equation with advection to move in transportation speed ρ. The boundary conditions describe a closed system in the production field. The adiabatic state in thermodynamics represents the same state [11].

With respect to the production flow system, generally, low volumes of a wide variety of products are produced through several stages in the production process. This method is good for producing specific control equipment such as semiconductor manufacturing equipment in our experience. We have reported many research findings in this area. The production flow process has nonlinear characteristics [12]. Moreover, we have made it clear that the manufacture of products proceeds in multiple stages from the beginning of production. Such volatility is encountered in every stage of manufacturing, and delays in the production line propagate this volatility to the successive steps. A delay in the production process is equivalent to a "fluctuation" in physical phenomena [13].

To achieve the production system goals, we propose the use of a mathematical model that focuses on the selection process and adaptation mechanism of the production lead time [14]. We model the throughput time of the production demand/production system in the production stage by using a stochastic differential equation of the log-normal type, which is derived from its dynamic behavior. Using this model and risk-neutral integral, we define and compute the evaluation equation for the compatibility condition of the production lead time. Furthermore, we apply the synchronization process and show that the throughput of the production process is reduced [14, 15].

In accordance with this result, we show that Kalman filter theory, conventionally used in state estimation problems in control theory, can be applied under an incomplete information state. In addition, by applying a theory of ongoing assessment in real option, the conditions that determine throughput rate are clarified and confirmed by numerical value calculations [15].

In this study, using the phase difference in the gradient system of an autonomous distributed system, we report that the production flow process is an excellent production method. Specifically, the variation between processes is examined as the synchronism between processes, which is regarded as the phase difference in the gradient system of an autonomous distributed system. In our previous study, we applied offset time in a joint model of an autonomous distributed system to the production process using a diffusion equation for the propagation of production elements and same physical quantity of propagation [11]. The present study extends to potential energy based on the offset time.

Further, from the obtained production flow process data, we introduce potential energy and show that if the production process cannot maintain a synchronous status, the bilateral symmetry of the potential function collapses. The synchronous process corresponds to Test−run2 in the production flow process. In contrast, in the case of asynchronous status, the bilateral symmetry of the potential function is maintained. An asynchronous process corresponds to Test−run1 in the production flow process. To the best of our knowledge, the application of phase difference in the gradient system of an autonomous distributed system has not been previously applied to the production process.

2. **Distribution System and Diffusion Equation of the Production Process.** From Figure 1, we refer to the network capacity (i.e., a statically acceptable amount of production) in an interprocess network (a production field) as R. An interprocess network indicates a sequential flow from one process to the other after the completion of the current process. Here assuming that the production density function for the i-th equipment is $S_i(x,t)$, $S_i(x,t)$ is expressed by

$$[J(x,t)dt - J(x+dx,t)dt]R = [S_i(x,t+dt) - S_i(x,t)]Rdx \tag{2.1}$$

where J is the production flow [11].

Next, we define the production flow as the displacement of a production density function in the unit production direction. In other words, the production density function is proportional to the cost necessary for production, and thus, it can be considered as the production cost per unit production. Furthermore, because production leads to a return, the production density function can be considered as a return density function

$$\frac{\partial S_i(x,t)}{\partial t} = D\frac{\partial^2 S_i(x,t)}{\partial x^2} \tag{2.2}$$

where D is the diffusion coefficient, t is the time variable, and x is the spatial variable.

This equation is equivalent to the diffusion equation derived from the minimization condition of free energy in a production field, indicating that the connections between processes can be treated as a diffusive propagation of products (refer to Figure 1) [11].

A model of the production process, which is connected in one dimension, is described as follows. The process of production is indicated by the movement of production units from one process (node) to another. This production flow is equivalent to transmission rate, which is defined as the rate of data flow between connected nodes in communication engineering. Accordingly, we formulate the production model in a manner similar to heat propagation in physics. Thus, the production process is modeled mathematically using a continuous diffusion type of partial differential equation consisting of time and spatial variables [11].

Setting the network capacity (the available static production volume) to R in an interprocess network (production field, equivalent to a stochastic field), we obtain the following:

$$[J(x)dt - J(X+dx)dt]R = [S(t+dt) - S(t)]Rdx \tag{2.3}$$

where J is the production flow and S is the production density.

In the present model, the production flow indicates the displacement of production processes in the direction related to the production density. In other words, the production cost per production is as follows:

Definition 2.1. *Production cost per unit production*

$$J = -D\frac{\partial S}{\partial x} \tag{2.4}$$

where D is a diffusion coefficient.

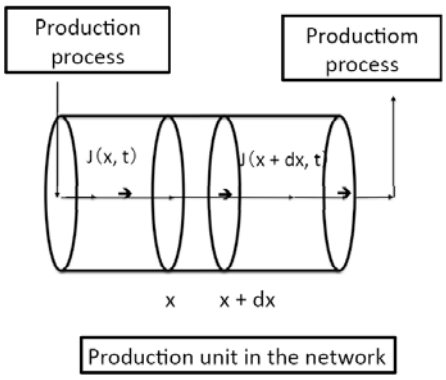

FIGURE 1. Network inter-process division of worker

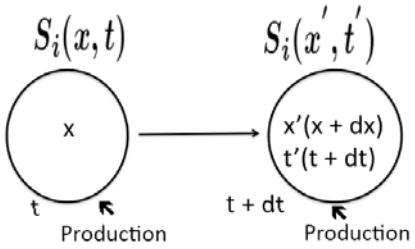

FIGURE 2. Unit of production by changing the excitation force

From Equation (2.3), we obtain

$$-\frac{\partial J}{\partial x} = \frac{\partial S}{\partial t} \tag{2.5}$$

From Equations (2.4) and (2.5), we obtain

$$\frac{\partial S}{\partial t} = D\frac{\partial^2 S}{\partial x^2} \tag{2.6}$$

where $t \in [0,T]$, $x \in [0,L] \equiv \Omega$, $S(0,x) = S_0(x)$, $B_x S(t,x)|_{x=\partial\Omega}$.

This equation is equivalent to the diffusion equation derived from the minimization condition of free energy in a production field [11]. The connections between processes can be treated as a diffusive propagation of products (refer to Figure 1). Please refer to our previous paper for details [11].

As shown in Figure 2, X represents the production elements that constitute a unit production and varies $X \to X'$ at $[t + dt]$. In other words, the unit production varies by exciting the external force and is the basis for revenue generation (an increase of potential energy). Therefore, in the transition $S_i(t,x) \to S_i(t,x')$, the production cost, which is the cumulated external force, increases. The connections between production processes are referred to as "joints".

In the general idea of production flow, we define the joint propagation model at multiple stages in the production process and the potential energy in the production field.

Thereafter, we can construct a control system, which increases the process throughput, by calculating the gradient function in the autonomous distributed system. The gradient function is described in the next section.

3. **Production Flow Process.** Figure 3 depicts a manufacturing process that is termed as a production flow process. This manufacturing process is employed in the production of control equipment. In this example, the production flow process consists of six stages. In each step S1-S6 of the manufacturing process, materials are being produced.

The direction of the arrows represents the direction of the production flow. In this process, production materials are supplied through the inlet and the end-product is shipped from the outlet.

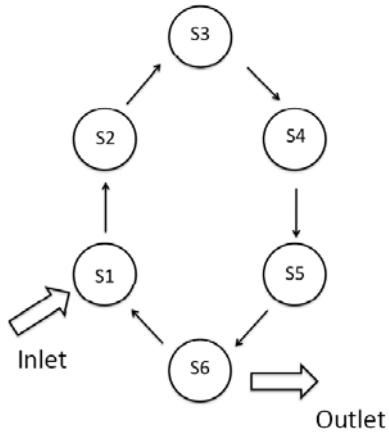

FIGURE 3. Production flow process

3.1. **Synchronous model.**

Definition 3.1. *The role of the synchronization model is to reduce the process throughput, i.e.,*

$$dS(t,x) = rS(t,x)dt + \sigma S(t,x)dW(t) \tag{3.1}$$

where $S(t,x)$ represents the production density function as a function of the synchronous status [10].

Synchronization minimizes the risk in the production process. To realize synchronization, we set the throughput of each stage to the same value. Because we set the working time for the workers in each work stage, there is no volatility in the working time between processes.

Here, $S(t,x)$ represents the production density function as a function of the synchronous status when the equipment is manufactured. t represents the manufacturing time. x represents the production process term when products are manufactured continuously. σ represents the volatility at each stage, and $W(t)$ represents the Wiener process. Please see our previous study on the detail analysis [10].

3.2. **Asynchronous model.**

Definition 3.2. *When we use the asynchronous model to represent a dynamical system, the throughput is not reduced.*

$$d\tilde{S}(t,x) = \bar{C}(t,x)\tilde{S}(t,x)dt + \tilde{\sigma}\tilde{S}(t,x)dW(t) \tag{3.2}$$

where $\bar{C}(t,x)$ represents the average working time of the total processes when the equipment is manufactured using an asynchronous process [10].

$$\bar{C}(t,x) = E[C(t,x)] = E\left[\sup_{t\in[0,T]} ||C(t,x)||^p\right] < \infty, \;\; p > 2 \tag{3.3}$$

where, $C(t,x)$ exists uniquely. Therefore, it is clear that Equation (3.3) is established. $C(t,x)$ is the arbitrage-free term under the equivalent martingale measure.

Therefore, each stage of the production flow process can be represented by the Wiener process. Because, the working time in each stage fluctuates stochastically, then, the

relative production density $\tilde{S}(t,x)$ is expressed as follows [21]:

$$\tilde{S}(t,x) = \tilde{S}(0,x) - \int_0^t \tilde{S}(u,x)\sigma_u^* \mathbf{1}_{T-u} d\hat{W}(t) \tag{3.4}$$

That is, the volatility σ_u^* exists. Then $\tilde{S}(t,x)$ is

$$\tilde{S}(t,x) = \frac{S(t,x)}{S(t,0)} \exp\left\{ \int_0^t r_u du - \int_0^t C(t,u) du \right\} \tag{3.5}$$

Therefore, according to Equations (3.3) and (3.4), the solution of $\tilde{S}(t,x)$ is as follows (asynchronous model):

$$\tilde{S}(t,x) = \tilde{S}(t,0) \exp\left\{ \left(r_c - \frac{1}{2}\sigma_c^2 \right) t + \sigma_c W(t) \right\} \tag{3.6}$$

$$d\tilde{S}(t,x) = r_c \tilde{S}(t,x) dt + \sigma_c \tilde{S}(t,x) d\hat{W}(t) \tag{3.7}$$

$\tilde{S}(t,x)$ is a martingale with respect to F_t [21].

Therefore, $\tilde{S}(t,x)$ satisfies Equation (3.2) (asynchronous model). Please see our previous study on the detail analysis [10].

4. Results of Test−run.

4.1. **Result of Test−run1.** Test−run1 is asynchronous process. Therefore, the throughput at each step of Test−run1 is different, the throughput of the entire stage becomes stochastic. Moreover, the stochastic throughput, which is a function of the current time and time remaining until the end of the stage, affects the performance of the entire system. In Tables 2 and 3, we present data that validates our findings presented above.

Therefore, the ratio of the measured throughput to the target throughput is considered as the drift term r_u^c in Equation (3.7). The fluidity of the system is affected by the throughput at each stage. In other words, because the manufacturing progress is affected by bottlenecks, the drift term r_u^c can be defined using the stochastic throughput [10].

Here the drift term r_u^c is

$$r_u^c = \frac{4.4}{6} \quad (0.73) \tag{4.1}$$

$$r_u^c = \frac{5.5}{6} \quad (0.92) \tag{4.2}$$

The required theoretical throughput for six pieces of equipment/day is computed in Equation (4.1). However, the actual throughput corresponds to 4.4 pieces of equipment/day.

Furthermore, we can use the same approach to compute the volatility of the throughput at each stage. This average of volatility is given as follows:

$$\sigma_s \approx 0.29 \left(= \frac{1}{N} \sum_{i=1}^{N} \sigma^i(x) \right) \tag{4.3}$$

Therefore,

Definition 4.1. *The system throughput in this model (production evaluation model)*

$$d\tilde{S}(t,x) = 0.73\tilde{S}(t,x)dt + 0.29\tilde{S}(t,x)d\hat{W}(t) \tag{4.4}$$

4.2. **Result of Test−run2.** Next, we consider the case of Test−run2.

Test−run2 is synchronous process. In this case, the process is set in such a way that each stage has the same throughput. Therefore, no risks are introduced as the process progresses. Hence, in principle, the throughput at each stage satisfies the condition. Moreover, because the manufacturing processes require synchronization, we can easily define the "synchronization throughput" [10].

This system has essentially no risk. However, in Tables 4 and 5 we do not observe any values of volatility equal to zero. Therefore, in Equation (3.1), the term σ is equal to the average volatility.

Here, r, σ in Equation (3.1) are

$$r^1 = \frac{5.5}{6} = 0.92$$
$$r^2 = 1 - 0.06 = 0.94$$

r^1 and r^2 are not much different. The volatility is

$$\sigma = 0.06$$

Therefore, the throughput model of this system is defined as follows.

Definition 4.2.

$$dS(t,x) = 0.92S(t,x)dt + 0.06S(t,x)dW(t) \tag{4.5}$$

If the system approaches the synchronization, $\sigma \to 1$. If $\sigma \to$ small data ($\sigma = 0.01$), this system becomes stationary.

For the case of a fully synchronized system, see Figure 4. In Figure 5, the integrated finite number of processing stages progresses depending on the synchronization throughput of each stage (stationary system).

Specifically, the synchronous production system is the principle, and the processing stages progress in a cycle, i.e., we set the throughput at T_1, T_2 and T_3 in Figure 6, and synchronize the stages in a cycle.

If Equation (4.6) is satisfied,

$$\frac{1}{N}\sum_{i=1}^{N} r_i^c \leq \sup\ r_i^c : \quad (i = 1, 2, \cdots, N) \tag{4.6}$$

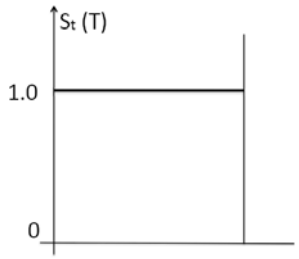

FIGURE 4. Perfect synchronization system

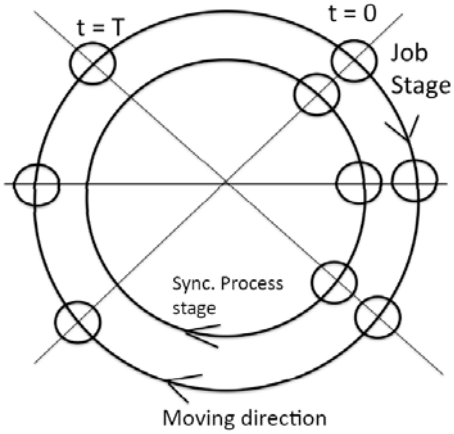

FIGURE 5. Perfect synchronization system

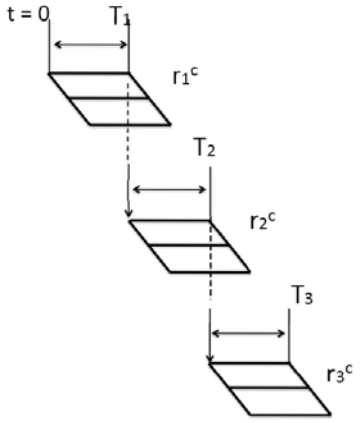

FIGURE 6. Cyclic synchronization

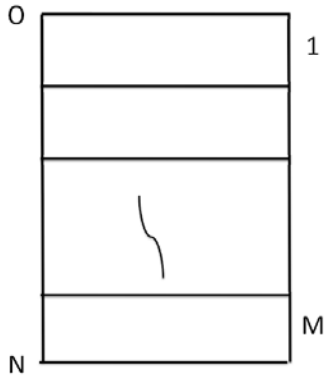

FIGURE 7. Concept of number of M cycle

a risk reduction system was constructed, where $N = kM$ $(k = 1, 2, \cdots, N)$ (k is a positive integer). Because we set the working time for the workers in each work stage, there is no volatility in the working time between processes.

Next, we applied the throughput model and used the results of the test runs to perform numerical calculations. Our model shows that the throughput for each process at each stage is satisfied. If Equation (6.3) is satisfied, r_i^c $(i = 1, 2, \cdots, N)$ is a real number. This process is a type of bottleneck synchronization. The bottleneck synchronization means a recommendation from the famous "The theory of constraints (TOC)" [9].

1. If $r_i^c \neq r_j^c$, $i \neq j$, synchronization of every stage.
2. $$\frac{1}{N}\sum_{i=1}^{c} r_i^c \leq \sup\ r_i^c, \quad i = 1, 2, \cdots, N \tag{4.7}$$
   if Equation (6.3) is satisfied, the process is a type of bottleneck synchronization.
3. $r_i^c = r_j^c$, $i = j < N$, the synchronization of some stages.

Here Figure 6 can be considered for item 3.

Definition 4.3. *Evaluation of the relative production density function $\tilde{S}_T(x)$ at $t = T$.*

$$d\tilde{S}(T, x) = r_t^c \tilde{S}(T, x)dt + \sigma_s^* \tilde{S}(T, x)d\hat{W}_t \tag{4.8}$$

In this case, the reduction of σ_s^* is a key point of building the system. Therefore, we named to "Synchronization with preprocess" method as to reduce this σ_s^*.

5. Analysis of the Test−run Results.

- (Test−run1): Each throughput in every process (S1-S6) is asynchronous, and its process throughput is asynchronous. Table 2 represents the production time (min) in each process. The volatilities of K3 and K8 increases due to the delay of K3 and K8 in Table 3. K3 and K8 of workers in Table 2 indicate the delay propagation of working time through S1-S6 stages. Table 3 represents the volatility in each process performed by workers. Table 2 represents the target time, and the theoretical throughput is given by $3 \times 199 + 2 \times 15 = 627$(min).

  In addition, the total working time in stage S3 is 199(min), which causes a bottleneck. Figure 8 is a graph illustrating the measurement data in Table 2, and it represents the total working time for each worker (K1-K9). The graph in Figure 9 represents the volatility data for each working time in Table 2.

TABLE 1. Correspondence between the table labels and the Test−run number

	Table Number	Production process	Working time	volatility
Test−run1	Table 2	Asynchronous process	627(min)	0.29
Test−run2	Table 4	Synchronous process	500(min)	0.06

TABLE 2. Total production time at each stages for each worker (asynchronous)

	WS	S1	S2	S3	S4	S5	S6
K1	15	20	20	25	20	20	20
K2	20	22	21	22	21	19	20
K3	10	20	26	25	22	22	26
K4	20	17	15	19	18	16	18
K5	15	15	20	18	16	15	15
K6	15	15	15	15	15	15	15
K7	15	20	20	30	20	21	20
K8	20	29	33	30	29	32	33
K9	15	14	14	15	14	14	14
Total	145	172	184	199	175	174	181

TABLE 3. Volatility of Table 2

K1	1.67	1.67	3.33	1.67	1.67	1.67
K2	2.33	2	2.33	2	1.33	1.67
K3	1.67	3.67	3.33	2.33	2.33	3.67
K4	0.67	0	1.33	1	0.33	1
K5	0	1.67	1	0.33	0	0
K6	0	0	0	0	0	0
K7	1.67	1.67	5	1.67	2	1.67
K8	4.67	6	5	4.67	5.67	6
K9	0.33	0.33	0	0.33	0.33	0.33

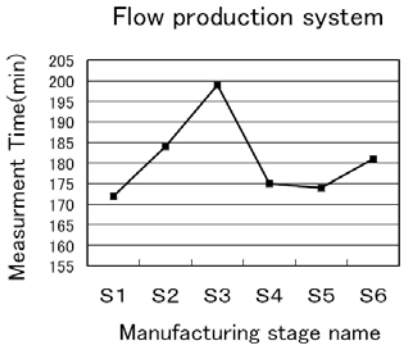

FIGURE 8. Total production time at each stage for each worker

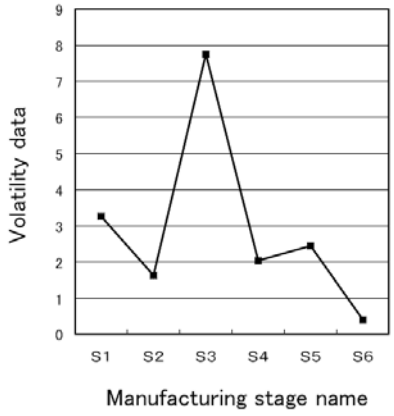

FIGURE 9. Volatility data at each stage for each worker

- (Test−run2): The target time in Table 4 is 500(min), and the theoretical throughput (not including the synchronized idle time) is 400(min). Table 5 represents the volatility data of each working process (S1-S6) for each worker (K1-K9).

In Table 1, Test−run2 is a good method in throughput clearly than Test−run1, and also that the volatility in the work (Test−run2) is less than the volatility (Test−run1).

6. **Applying Offset to the Production Flow Process.** We represent the offset time between processes i and j as well as the traffic signal control as follows. The phase difference corresponds to the standard deviation as a new suggestion. From Figure 12, we can derive the following:

$$\frac{d\theta_i}{dt} = \omega_i \tag{6.1}$$

TABLE 4. Total production time at each stage for each worker (synchronous)

	WS	S1	S2	S3	S4	S5	S6
K1	20	20	24	20	20	20	20
K2	20	20	20	20	20	22	20
K3	20	20	20	20	20	20	20
K4	20	25	25	20	20	20	20
K5	20	20	20	20	20	20	20
K6	20	20	20	20	20	20	20
K7	20	20	20	20	20	20	20
K8	20	27	27	22	23	20	20
K9	20	20	20	20	20	20	20
Total	180	192	196	182	183	182	180

TABLE 5. Volatility of Table 4

K1	0	1.33	0	0	0	0
K2	0	0	0	0	0.67	0
K3	0	0	0	0	0	0
K4	1.67	1.67	0	0	0	0
K5	0	0	0	0	0	0
K6	0	0	0	0	0	0
K7	0	0	0	0	0	0
K8	2.33	2.33	0.67	1	0	0
K9	0	0	0	0	0	0

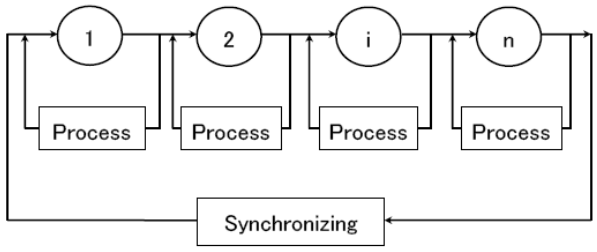

FIGURE 10. Connection of production system cascaded by N processes

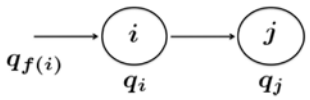

FIGURE 11. Transition of production stage

From Equation (6.1),

$$\frac{d}{dt}(\theta_i - \theta_j) = \omega_i - \omega_j \tag{6.2}$$

If $\omega_i = \omega_j$, $d/dt(\theta_i - \theta_j) = 0$. Here the relationship between the offset T_{ij} and phase difference $(\theta_i - \theta_j)$ is

$$T_{ij} = \frac{\theta_i - \theta_j}{\omega_i} \tag{6.3}$$

Definition 6.1. *Offset* T_{ij}

$$T_{ij} = \frac{\phi(i,j)}{\omega_i} \tag{6.4}$$

where $\phi(i,j)$ *is the phase difference and* ω_i *is the target throughput (read time).*

To address these considerations, Yuasa and Ito have proposed a structural theory. We have attempted to apply the proposed method to a production system in accordance with this theory [18, 19].

Here we briefly summarize the structural theory of the autonomous distributed system proposed by Yuasa and Ito.

The system model for the process i is

$$\frac{d\theta_i}{dt} = f_i(\theta_{i1}, \theta_{i2}, \theta_{i3}, \cdots, \theta_{im}) \tag{6.5}$$

where $\theta_{i1}, \theta_{i2}, \cdots, \theta_{im}$ is the phase of process coupling with θ_i.

The matrix $\mathbf{A}$ between the state of the phase difference $\varphi \equiv (\varphi_1, \varphi_2, \cdots, \varphi_N)$ and the state $\theta \equiv \{\theta_1, \theta_2, \cdots, \theta_n\}$ is assumed as follows:

Assumption 1.

$$\varphi = \mathbf{A}^{\mathbf{t}}\theta \tag{6.6}$$

where t indicates the transposed matrix and $\mathbf{A}$ is the "incident matrix" in graph theory.

From Equations (6.5) and (6.6),

$$\frac{d\varphi}{dt} = \mathbf{A}^{\mathbf{t}}\mathbf{f} \tag{6.7}$$

We obtain the dynamic model of the state difference φ.

For this discussion, let φ be autonomous; that is, the necessary and sufficient conditions under which $\mathbf{A}^{\mathbf{t}}\mathbf{f}$ satisfies only the function φ are as follows [17, 18, 19].

Lemma 6.1. *Any i, j*

$$\sum_{k=1}^{n} \frac{\partial \varphi_i}{\partial \theta_k} = \sum_{k=1}^{n} \frac{\partial \varphi_j}{\partial \theta_k} \tag{6.8}$$

To prove this lemma, θ is defined in an n-dimensional space. However, φ in an $(n-1)$-dimensional space is defined as follows:

$$\phi = \sum_{i=1}^{n} \theta_i \tag{6.9}$$

ϕ, which is orthogonal to space φ, does not become an element of $\mathbf{A}^{\mathbf{t}}\mathbf{f}$; that is, $\mathbf{A}^{\mathbf{t}}\mathbf{f}$ does not become a function of ϕ.

Definition 6.2. *Variable of state φ_{i_k} difference between θ_{i_k} and θ_i*

$$\varphi_{i_k} = \theta_{i_k} - \theta_i \tag{6.10}$$

The necessary and sufficient conditions under which φ satisfies the gradient system are as follows:

$$\begin{aligned} \frac{d\varphi_i}{dt} &= f_i(\varphi_i) \\ \varphi_i &= \sum_{k=1}^{m_i} (\theta_{i_k} - \theta_i) \end{aligned} \tag{6.11}$$

The potential function to be formed in space φ is as follows:

$$V(\varphi) = \sum_{i=1}^{n} \int f_i(\varphi_i) d\varphi_i \tag{6.12}$$

The potential structure is derived from the sum of the local potentials. Therefore, in equipment production, such as in a production flow system, each process (subsystem) has a unique potential structure. In addition, each process model becomes a nonlinear structure by the interaction between processes. The total potential is the sum of the local potentials of each process, and the structure of the autonomous distributed system can only be unique when the total potential is the sum of the local potentials [18, 19].

Here we describe the basic production model, such as the production flow process shown in Figure 3. According to form of the phase, such as those Figure 12 and Figure 13, which are related to process size and manpower ability within a process, each process

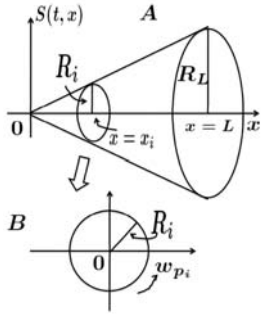

FIGURE 12. Production density function and progress of production process

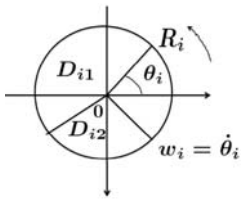

FIGURE 13. Relationship between angular frequency and angular

demonstrates phase difference. If this phase difference can be measured in Figure 13, the offset between the processes can be defined by Equation (6.4).

On the basis of the above gradient system, the production process is constructed as follows.

Assumption 2.

$$\frac{d\theta_i}{dt} = -\frac{\delta W_i^p(\theta_i)}{\delta \theta_i} + \omega_i \tag{6.13}$$

where W_i^p is as follows:

$$W_i^p(\theta_i) = -\Big[\beta\Big(\frac{q_{f(i)} + q_j}{q_i}\Big)\Big]\cos\{\phi(i,j) - D(i,j)\} \tag{6.14}$$

where $q_{f(i)}$ indicates the production volume of the forward process and q_j indicates the production volume of the next process after process i.

$$\phi(i,j) = \theta_i - \theta_j \tag{6.15}$$

Therefore, we can construct the gradient system as follows:

$$\frac{d\theta_i}{dt} = \omega_i - 2\Big[\beta\Big(\frac{q_{f(i)} + q_j}{q_i}\Big)\Big]\sin\{\phi(i,j) - D(i,j)\} \tag{6.16}$$

where, whenever $\phi(i,j) = D(i,j)$, W_i^p obtains its minimum value, and we obtain

$$\frac{d\theta_i}{dt} = \omega_i \tag{6.17}$$

Definition 6.3. $D(i,j)$

$$D(i,j) = \frac{q_j}{q_{f(i)} + q_i} \cdot \omega_i \cdot \frac{|L(i,j)|}{\rho} \tag{6.18}$$

where $q_{f(i)}$ is the throughput per unit process of process $f(i)$, q_i is the throughput per unit process of process i, q_j is the throughput per unit process, and ρ is the standard working time of each process.

Definition 6.4. *Average offset time value*

$$\text{Average } D(i,j) = \left\{\frac{\max(L(i,j)) + \min(L(i,j))}{2}\right\} \tag{6.19}$$

$$D(i,j) = \begin{cases} 0 & (q_i = q_j = 0) \\ \frac{q_j}{q_{f(i)}+q_i} D(i,j) & (\text{Other}) \end{cases} \tag{6.20}$$

We consider the one-way propagation.

$$D(i,j) = D(j,i) \tag{6.21}$$

At this time,

$$\sigma_i = \frac{|D_1|}{|D_1| + |D_2|} \tag{6.22}$$

$$\phi(i,j) = \Big[\Big\{\theta_i - \xi(i,(i,j))\Big\} - \Big\{\theta_j - \xi(i,(j,i))\Big\}\Big] \tag{6.23}$$

where if we assume that the production flow and volume do not have sudden fluctuations, the throughput converges to the local minimum point of the potential.

In other words, the phase difference $\phi(i,j)$ converges to $D(i,j)$. Therefore, if we set the value of $D(i,j)$, we can estimate the degree of process synchronization.

$$\begin{aligned} \frac{dx_i}{dt} &= f_{x_i}(x_i, y_i) + f_i \\ \frac{dy_i}{dt} &= f_{y_i}(x_i, y_i) + g_i \end{aligned} \tag{6.24}$$

The system model for the process i is as follows [18]:

$$\frac{dx_i}{dt} = -a_i y_i + \mu_i x_i (r_{oi}^2 - r_i^2) + f_i \tag{6.25}$$

$$\frac{dy_i}{dt} = a_i x_i + \mu_i y_i (r_{oi}^2 - r_i^2) + g_i \tag{6.26}$$

where $r_i^2 = x_i^2 + y_i^2$.

Equation (6.26) represents the model including the interaction between x_i and y_i. As can be seen in Figure 12, and Figure 13, each process has an initial phase difference as we run the unit process. By using polar coordinates for Equations (6.25) and (6.26), we obtain the following:

$$\frac{dr_i}{dt} = \mu_i r_i (r_{oi}^2 - r_i^2) + f_i c_i + g_i s_i \tag{6.27}$$

$$\frac{d\theta_i}{dt} = a_i - \frac{1}{r_i}(f_i s_i - g_i c_i), \quad {}^{\forall} \quad s_i = \sin\theta_i, \quad c_i = \cos\theta_i \tag{6.28}$$

The processes are connected by cascade coupling from process (1) through (n), each process having independent throughput, as can be seen in Figure 10. Here, the dynamic throughput model for the process is used by the oscillation model for autonomous work [18].

$$\frac{d\theta_i(t)}{dt} = \omega_i \tag{6.29}$$

Here we set the phase difference between i and j to φ_{ij}. We obtain the following:

$$\varphi_{i,j} = \theta_i - \theta_j \tag{6.30}$$

Therefore,

$$\begin{aligned} \frac{d\varphi_{i,j}}{dt} = \frac{d(\theta_i - \theta_j)}{dt} &= (a_i - a_j) - \frac{1}{r_i}(f_i s_i - g_i c_i) + \frac{1}{r_j}(f_j s_j - g_j c_j) \\ &= (a_i - a_j) + \Phi(\varphi_{i,j}) \end{aligned} \tag{6.31}$$

where

$$\Phi(\varphi_{i,j}) = \frac{1}{r_j}(f_j s_j - g_j c_j) - \frac{1}{r_i}(f_i s_i - g_i c_i) \tag{6.32}$$

Here Equation (6.30) represents the autonomous distributed system. From here, we can construct a gradient system [18].

Now, according to Equation (6.14) and by applying Yuasa's potential function, we can obtain the following [18]:

$$V(\varphi_{i,j}) = F\varphi_{i,j} + B(-4C\cos\varphi_{i,j} + \cos 2\varphi_{i,j}) \tag{6.33}$$

Therefore, the gradient system is as follows:

$$\frac{d\varphi_{i,j}}{dt} = -\frac{\partial V(\varphi_{i,j})}{\partial \varphi_{i,j}} = -F - B\Big\{4C\sin\varphi_{i,j} - 2\sin 2\varphi_{i,j}\Big\} \tag{6.34}$$

where $F \equiv Constant$, C is a synchronizing parameter, and B is a system parameter. The parameters C and F significantly affect the shape of the function $V(\varphi_{i,j})$. Similar to Equation (6.13), the gradient model is as follows:

$$\frac{d\theta_i}{dt} = \omega_i - \frac{\partial V(\theta_i)}{\partial \theta_i} \tag{6.35}$$

Then Equation (6.35) is rewritten as follows:

$$\begin{aligned}\frac{d\theta_i}{dt} &= \omega_i - \Big[B_i\Big\{4C_i\sin(\varphi_{i,j} - D(i,j)) - 2\sin 2(\varphi_{i,j} - D(i,j))\Big\} \\ &= \omega_i + B_i\Big\{-4C_i\sin(\varphi_{i,j} - D(i,j)) + 2\sin 2(\varphi_{i,j} - D(i,j))\Big\}\end{aligned} \tag{6.36}$$

Similar to Equations (6.35) and (6.36), we can control the stable phase difference by varying the value of C_i.

Based on Yuasa's reports, the interactions between f_i and g_i in Equation (6.29) have certain limitations and are deeply involved with the coefficient of the potential function. If Equation (6.31) is equivalent to Equation (6.34), we can obtain the following:

$$(a_i - a_j) + \Phi(\varphi_{i,j}) = -F - B\{4C\sin\varphi_{i,j} - 2\sin 2\varphi_{i,j}\} \tag{6.37}$$

From Equation (6.32), $\Phi(\varphi_{i,j})$ is described as follows:

$$\Phi(\varphi_{i,j}) = \frac{1}{r_j}(f_j\sin\theta_j - g_j\cos\theta_j) - \frac{1}{r_i}(f_i\sin\theta_i - g_i\cos\theta_i) \tag{6.38}$$

If we choose values for f_i and g_i appropriately, the function $\Phi(\varphi_{i,j})$ includes (B, C) [18, 19]. Therefore, if we set the potential function and system parameters (F, B, C) in Equation

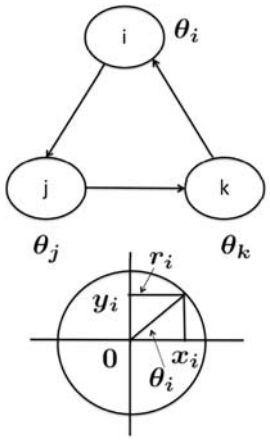

FIGURE 14. Production flow process by polar coordinate

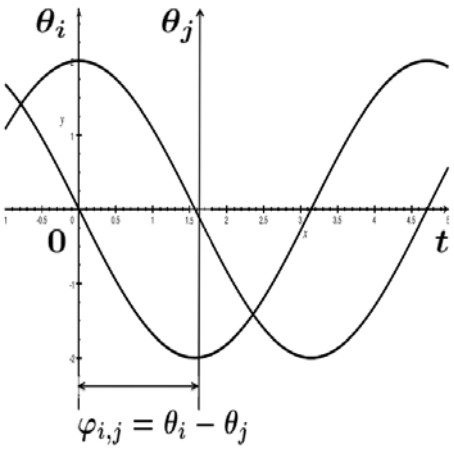

FIGURE 15. Phase difference of process i and process j

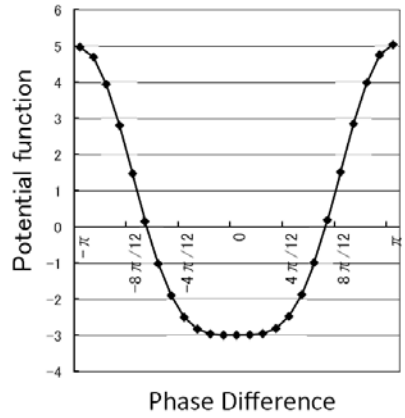

FIGURE 16. Value of potential function (F = 0.01, B = 1, C = 1.5) in Table 7

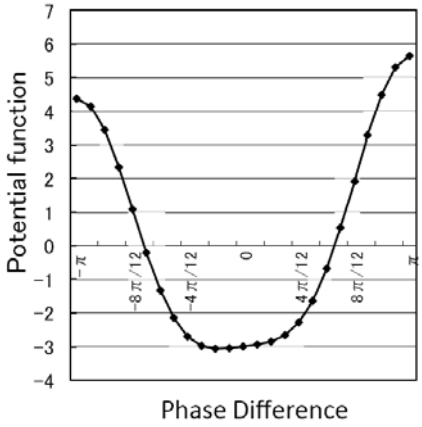

FIGURE 17. Value of potential function (F = 0.2, B = 1, C = 1.5) in Table 8

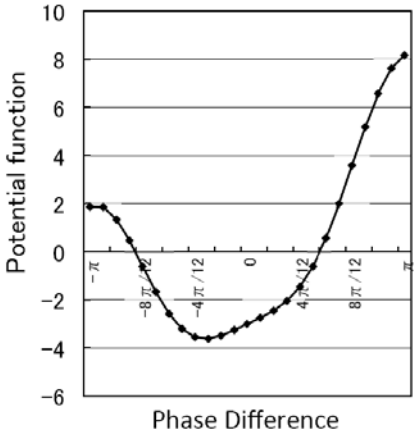

FIGURE 18. Value of potential function (F = 1, B = 1, C = 1.5) in Table 9

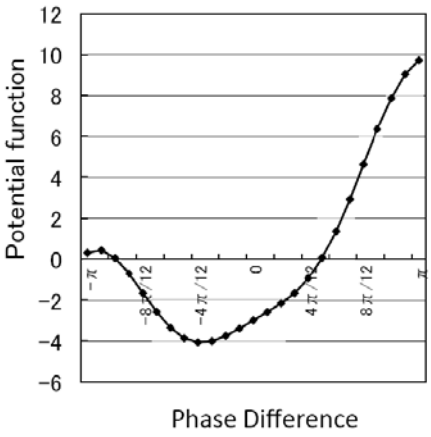

FIGURE 19. Value of potential function (F = 1.5, B = 1, C = 1.5) in Table 10

TABLE 6. Values of F, B, C for parameter 1-8 in potential function

	Table 7	Table 8	Table 9	Table 10	Table 11	Table 12	Table 13	Table 14
F	0.01	0.2	1	1.5	5.5	0.01	0.01	0.01
B	1	1	1	1	1	10	1	1
C	1.5	1.5	1.5	1.5	1.5	1.5	0.01	1.5

(6.33) appropriately, we can show the potential function in Figure 16, Figure 17, Figure 18, and Figure 19.

7. **Numerical Results.** We represent the variation status of workers in the stages using the potential function. According to Equation (6.33), we use Equation (7.1) for the numerical calculation. Equation (7.1) is a potential function that includes the constant term F. Figures 16-23 show the potential function with constant terms F, B, and C (Table 6). Tables 7-14 show the parameters of F, B and C versus D.

If we choose a significantly large value, the process deviates from synchronization, i.e., if $|F| \geq 3\sqrt{3}B$, the process cannot be synchronized [18]. We refer to Yuasa's report for the numerical simulations. From Figures 16-23, it is evident that F = 0.01 does not

TABLE 7. Parameter value of F, B, C, D (1-25) in potential function

	1	2	3	4	5	6	7	8	9	10	11	12	
F	0.01	0.01	0.01	0.01	0.01	0.01	0.01	0.01	0.01	0.01	0.01	0.01	
B	1	1	1	1	1	1	1	1	1	1	1	1	
C	1	1	1	1	1	1	1	1	1	1	1	1	
D	$-\pi$	$-(11/12)\pi$	$-(10/12)\pi$	$-(9/12)\pi$	$-(8/12)\pi$	$-(7/12)\pi$	$-(6/12)\pi$	$-(5/12)\pi$	$-(4/12)\pi$	$-(3/12)\pi$	$-(2/12)\pi$	$-(1/12)\pi$	
	13	14	15	16	17	18	19	20	21	22	23	24	25
F	0.01	0.01	0.01	0.01	0.01	0.01	0.01	0.01	0.01	0.01	0.01	0.01	0.01
B	1	1	1	1	1	1	1	1	1	1	1	1	1
C	1	1	1	1	1	1	1	1	1	1	1	1	1
D	0	$(1/12)\pi$	$(2/12)\pi$	$(3/12)\pi$	$(4/12)\pi$	$(5/12)\pi$	$(6/12)\pi$	$(7/12)\pi$	$(8/12)\pi$	$(9/12)\pi$	$(10/12)\pi$	$(11/12)\pi$	π

TABLE 8. Parameter value of F, B, C, D (1-25) in potential function

	1	2	3	4	5	6	7	8	9	10	11	12	
F	0.2	0.2	0.2	0.2	0.2	0.2	0.2	0.2	0.2	0.2	0.2	0.2	
B	1	1	1	1	1	1	1	1	1	1	1	1	
C	1	1	1	1	1	1	1	1	1	1	1	1	
D	$-\pi$	$-(11/12)\pi$	$-(10/12)\pi$	$-(9/12)\pi$	$-(8/12)\pi$	$-(7/12)\pi$	$-(6/12)\pi$	$-(5/12)\pi$	$-(4/12)\pi$	$-(3/12)\pi$	$-(2/12)\pi$	$-(1/12)\pi$	
	13	14	15	16	17	18	19	20	21	22	23	24	25
F	0.2	0.2	0.2	0.2	0.2	0.2	0.2	0.2	0.2	0.2	0.2	0.2	0.2
B	1	1	1	1	1	1	1	1	1	1	1	1	1
C	1	1	1	1	1	1	1	1	1	1	1	1	1
D	0	$(1/12)\pi$	$(2/12)\pi$	$(3/12)\pi$	$(4/12)\pi$	$(5/12)\pi$	$(6/12)\pi$	$(7/12)\pi$	$(8/12)\pi$	$(9/12)\pi$	$(10/12)\pi$	$(11/12)\pi$	π

TABLE 9. Parameter value of F, B, C, D (1-25) in potential function

	1	2	3	4	5	6	7	8	9	10	11	12	
F	1	1	1	1	1	1	1	1	1	1	1	1	
B	1	1	1	1	1	1	1	1	1	1	1	1	
C	1	1	1	1	1	1	1	1	1	1	1	1	
D	$-\pi$	$-(11/12)\pi$	$-(10/12)\pi$	$-(9/12)\pi$	$-(8/12)\pi$	$-(7/12)\pi$	$-(6/12)\pi$	$-(5/12)\pi$	$-(4/12)\pi$	$-(3/12)\pi$	$-(2/12)\pi$	$-(1/12)\pi$	
	13	14	15	16	17	18	19	20	21	22	23	24	25
F	1	1	1	1	1	1	1	1	1	1	1	1	1
B	1	1	1	1	1	1	1	1	1	1	1	1	1
C	1	1	1	1	1	1	1	1	1	1	1	1	1
D	0	$(1/12)\pi$	$(2/12)\pi$	$(3/12)\pi$	$(4/12)\pi$	$(5/12)\pi$	$(6/12)\pi$	$(7/12)\pi$	$(8/12)\pi$	$(9/12)\pi$	$(10/12)\pi$	$(11/12)\pi$	π

TABLE 10. Parameter value of F, B, C, D (1-25) in potential function

	1	2	3	4	5	6	7	8	9	10	11	12	
F	1.5	1.5	1.5	1.5	1.5	1.5	1.5	1.5	1.5	1.5	1.5	1.5	
B	1	1	1	1	1	1	1	1	1	1	1	1	
C	1	1	1	1	1	1	1	1	1	1	1	1	
D	$-\pi$	$-(11/12)\pi$	$-(10/12)\pi$	$-(9/12)\pi$	$-(8/12)\pi$	$-(7/12)\pi$	$-(6/12)\pi$	$-(5/12)\pi$	$-(4/12)\pi$	$-(3/12)\pi$	$-(2/12)\pi$	$-(1/12)\pi$	
	13	14	15	16	17	18	19	20	21	22	23	24	25
F	1.5	1.5	1.5	1.5	1.5	1.5	1.5	1.5	1.5	1.5	1.5	1.5	1.5
B	1	1	1	1	1	1	1	1	1	1	1	1	1
C	1	1	1	1	1	1	1	1	1	1	1	1	1
D	0	$(1/12)\pi$	$(2/12)\pi$	$(3/12)\pi$	$(4/12)\pi$	$(5/12)\pi$	$(6/12)\pi$	$(7/12)\pi$	$(8/12)\pi$	$(9/12)\pi$	$(10/12)\pi$	$(11/12)\pi$	π

affect the shape of the potential function. However, F = 0.2 or more affects the shape of the potential function, and the symmetric potential function collapses. In other words, the production process cannot maintain the synchronous status. However, B does not affect the symmetric potential function significantly. C also does not affect the symmetric potential function; however, the stabilization period is shortened by setting a smaller value, i.e., C = 0.01.

$$V_F = F \times D + B \times (-4 \times C \cos(D) + \cos(2D)) \tag{7.1}$$

8. **Conclusions.** The phase difference between stages in a process corresponds to the standard deviation of working time. When the phase difference is constant, the total throughput can be minimized. We show that a synchronous process can be realized by

TABLE 11. Parameter value of F, B, C, D (1-25) in potential function

	1	2	3	4	5	6	7	8	9	10	11	12	
F	5.5	5.5	5.5	5.5	5.5	5.5	5.5	5.5	5.5	5.5	5.5	5.5	
B	1	1	1	1	1	1	1	1	1	1	1	1	
C	1	1	1	1	1	1	1	1	1	1	1	1	
D	$-\pi$	$-(11/12)\pi$	$-(10/12)\pi$	$-(9/12)\pi$	$-(8/12)\pi$	$-(7/12)\pi$	$-(6/12)\pi$	$-(5/12)\pi$	$-(4/12)\pi$	$-(3/12)\pi$	$-(2/12)\pi$	$-(1/12)\pi$	
	13	14	15	16	17	18	19	20	21	22	23	24	25
F	5.5	5.5	5.5	5.5	5.5	5.5	5.5	5.5	5.5	5.5	5.5	5.5	5.5
B	1	1	1	1	1	1	1	1	1	1	1	1	1
C	1	1	1	1	1	1	1	1	1	1	1	1	1
D	0	$(1/12)\pi$	$(2/12)\pi$	$(3/12)\pi$	$(4/12)\pi$	$(5/12)\pi$	$(6/12)\pi$	$(7/12)\pi$	$(8/12)\pi$	$(9/12)\pi$	$(10/12)\pi$	$(11/12)\pi$	π

TABLE 12. Parameter value of F, B, C, D (1-25) in potential function

	1	2	3	4	5	6	7	8	9	10	11	12	
F	0.01	0.01	0.01	0.01	0.01	0.01	0.01	0.01	0.01	0.01	0.01	0.01	
B	10	10	10	10	10	10	10	10	10	10	10	10	
C	1	1	1	1	1	1	1	1	1	1	1	1	
D	$-\pi$	$-(11/12)\pi$	$-(10/12)\pi$	$-(9/12)\pi$	$-(8/12)\pi$	$-(7/12)\pi$	$-(6/12)\pi$	$-(5/12)\pi$	$-(4/12)\pi$	$-(3/12)\pi$	$-(2/12)\pi$	$-(1/12)\pi$	
	13	14	15	16	17	18	19	20	21	22	23	24	25
F	0.01	0.01	0.01	0.01	0.01	0.01	0.01	0.01	0.01	0.01	0.01	0.01	0.01
B	10	10	10	10	10	10	10	10	10	10	10	10	
C	1	1	1	1	1	1	1	1	1	1	1	1	1
D	0	$(1/12)\pi$	$(2/12)\pi$	$(3/12)\pi$	$(4/12)\pi$	$(5/12)\pi$	$(6/12)\pi$	$(7/12)\pi$	$(8/12)\pi$	$(9/12)\pi$	$(10/12)\pi$	$(11/12)\pi$	π

TABLE 13. Parameter value of F, B, C, D (1-25) in potential function

	1	2	3	4	5	6	7	8	9	10	11	12	
F	0.01	0.01	0.01	0.01	0.01	0.01	0.01	0.01	0.01	0.01	0.01	0.01	
B	1	1	1	1	1	1	1	1	1	1	1	1	
C	0.01	0.01	0.01	0.01	0.01	0.01	0.01	0.01	0.01	0.01	0.01	0.01	0.01
D	$-\pi$	$-(11/12)\pi$	$-(10/12)\pi$	$-(9/12)\pi$	$-(8/12)\pi$	$-(7/12)\pi$	$-(6/12)\pi$	$-(5/12)\pi$	$-(4/12)\pi$	$-(3/12)\pi$	$-(2/12)\pi$	$-(1/12)\pi$	
	13	14	15	16	17	18	19	20	21	22	23	24	25
F	0.01	0.01	0.01	0.01	0.01	0.01	0.01	0.01	0.01	0.01	0.01	0.01	0.01
B	1	1	1	1	1	1	1	1	1	1	1	1	1
C	0.01	0.01	0.01	0.01	0.01	0.01	0.01	0.01	0.01	0.01	0.01	0.01	0.01
D	0	$(1/12)\pi$	$(2/12)\pi$	$(3/12)\pi$	$(4/12)\pi$	$(5/12)\pi$	$(6/12)\pi$	$(7/12)\pi$	$(8/12)\pi$	$(9/12)\pi$	$(10/12)\pi$	$(11/12)\pi$	π

TABLE 14. Parameter value of F, B, C, D (1-25) in potential function

	1	2	3	4	5	6	7	8	9	10	11	12	
F	0.01	0.01	0.01	0.01	0.01	0.01	0.01	0.01	0.01	0.01	0.01	0.01	
B	1	1	1	1	1	1	1	1	1	1	1	1	
C	1.5	1.5	1.5	1.5	1.5	1.5	1.5	1.5	1.5	1.5	1.5	1.5	1.5
D	$-\pi$	$-(11/12)\pi$	$-(10/12)\pi$	$-(9/12)\pi$	$-(8/12)\pi$	$-(7/12)\pi$	$-(6/12)\pi$	$-(5/12)\pi$	$-(4/12)\pi$	$-(3/12)\pi$	$-(2/12)\pi$	$-(1/12)\pi$	
	13	14	15	16	17	18	19	20	21	22	23	24	25
F	0.01	0.01	0.01	0.01	0.01	0.01	0.01	0.01	0.01	0.01	0.01	0.01	0.01
B	1	1	1	1	1	1	1	1	1	1	1	1	1
C	1.5	1.5	1.5	1.5	1.5	1.5	1.5	1.5	1.5	1.5	1.5	1.5	1.5
D	0	$(1/12)\pi$	$(2/12)\pi$	$(3/12)\pi$	$(4/12)\pi$	$(5/12)\pi$	$(6/12)\pi$	$(7/12)\pi$	$(8/12)\pi$	$(9/12)\pi$	$(10/12)\pi$	$(11/12)\pi$	π

the gradient system. To achieve autonomous synchronization in the individual stages of a process, it is most important to maintain the target throughput that has been set for each stage of the process.

Using actual production flow system data, we identified synchronous and asynchronous processes. If parameter F ≥ 0.2, the symmetric potential function collapses. The shape of the potential function is not affected by B = 10. In addition, C does not significantly affect the symmetric potential function; however, the stabilization period is shortened.

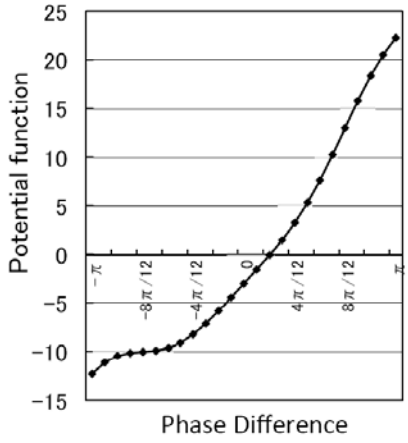

FIGURE 20. Value of potential function (F = 5.5, B = 1, C = 1.5) in Table 11

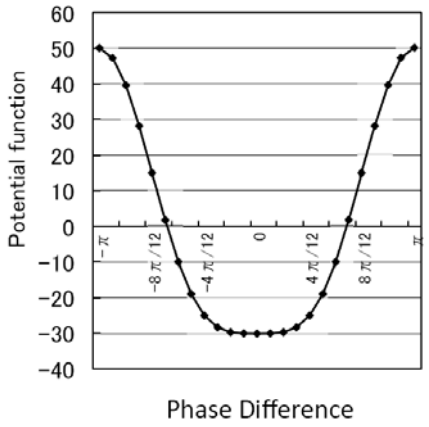

FIGURE 21. Value of potential function (F = 0.01, B = 10, C = 1.5) in Table 12

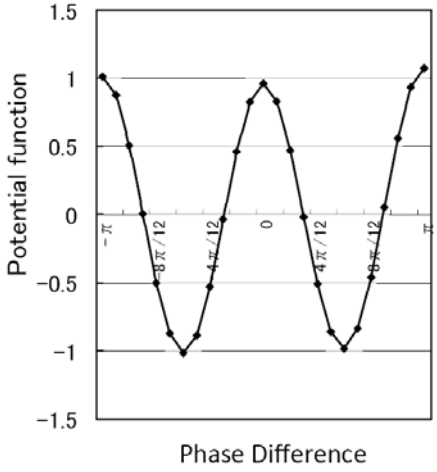

FIGURE 22. Value of potential function (F = 0.01, B = 1, C = 0.01) in Table 13

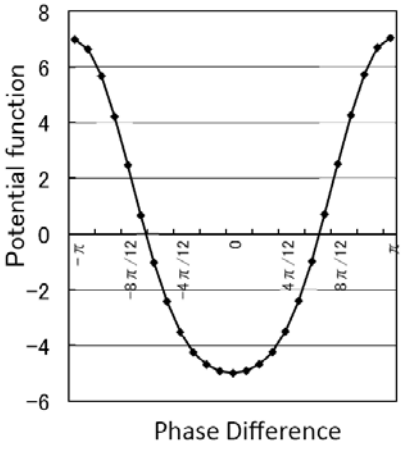

FIGURE 23. Value of potential function (F = 0.01, B = 1, C = 1.5) in Table 14

REFERENCES

[1] M. E. Mundel, Improving productivity and effectness, *Prentice-Hall*, NZ, 1983.

[2] R. E. Haber, A. Gajate, S. Y. Liang, R. Haber-Haber and R. M. del Toro, An optimal controller for a high-performance drilling process implemented over an industrial network, *International Journal of Innovative Computing, Information and Control*, vol.7, no.3, pp.1481-1498, 2011.

[3] K. Nishioka, Y. Mizutani, H. Ueno et al., Toward the integrated optimization of steel plate production process – A proposal for production control by multi-scale hierarchical modeling –, *Synthesiology*, vol.5, no.2, pp.98-112, 2012.

[4] L. Sun, X. Hu, Y. Fang and M. Huang, Knowledge representation for distribution problem in urban distribution systems, *International Journal of Innovative Computing, Information and Control*, vol.6, no.9, pp.4145-4156, 2010.

[5] L. Hu, D. Yue and J. Li, Availability analysis and design optimization for repairable series-parallel system with failure dependencies, *International Journal of Innovative Computing, Information and Control*, vol.8, no.10(A), pp.6693-6705, 2012.

[6] K. Shirai, Y. Amano, S. Omatu and E. Chikayama, Power-law distribution of rate-of-return deviation and evaluation of cash flow in a control equipment manufacturing company, *International Journal of Innovative Computing, Information and Control*, vol.9, no.3, pp.1095-1112, 2013.

[7] K. Shirai, Y. Amano and S. Omatu, Consideration of phase transition mechanisms during production in manufacturing processes, *International Journal of Innovative Computing, Information and Control*, vol.9, no.9, pp.3611-3626, 2013.
[8] K. Shirai and Y. Amano, Self-similarity of fluctuations for throughput deviations within a production process, *International Journal of Innovative Computing, Information and Control*, vol.10, no.3, pp.1001-1016, 2014.
[9] S. J. Baderstone and V. J. Mabin, A review Goldratt's theory of constraints (TOC) – Lessons from the international literature, *Operations Research Society of New Zealand the 33rd Annual Conference*, University of Auckland, New Zealand, 1998.
[10] K. Shirai, Y. Amano and S. Omatu, Improving throughput by considering the production process, *International Journal of Innovative Computing, Information and Control*, vol.9, no.12, pp.4917-4930, 2013.
[11] K. Shirai and Y. Amano, Production density diffusion equation propagation and production, *IEEJ Transactions on Electronics, Information and Systems*, vol.132-C, no.6, pp.983-990, 2012.
[12] K. Shirai and Y. Amano, Nonlinear characteristics of the rate of return in the production process, *International Journal of Innovative Computing, Information and Control*, vol.10, no.2, pp.601-616, 2014.
[13] K. Shirai, Y. Amano and S. Omatu, Propagation of working-time delay in production, *International Journal of Innovative Computing, Information and Control*, vol.10, no.1, pp.169-182, 2014.
[14] K. Shirai and Y. Amano, A study on mathematical analysis of manufacturing lead time – Application for deadline scheduling in manufacturing system, *IEEJ Transactions on Electronics, Information and Systems*, vol.132-C, no.12, pp.1973-1981, 2012.
[15] K. Shirai, Y. Amano and S. Omatu, Throughput analysis for manufacturing process by using a Kalman filter theory under uncertainty based on physical approach, *International Journal of Innovative Computing, Information and Control*, vol.9, no.11, pp.4431-4445, 2013.
[16] A. T. Winfree, *The Geometry of Biological Time*, Springer, 2001.
[17] M. Sugi, *Autonomous Decentralized Control of Traffic Signal Network by Reaction-Diffusion Equations on a Graph*, Ph.D. Thesis, 2002.
[18] M. Sugi, H. Yuasa and T. Arai, Autonomous decentralized control of traffic signal network by reaction-diffusion equations on a graph, *Journal of SICE*, vol.39, no.1, pp.51-58, 2003.
[19] Y. Maeda and T. Arai, Planning of graspless manipulation by a multifingered robot hand, *Advanced Robotics*, vol.19, no.5, pp.501-521, 2005.
[20] H. Tasaki, *Thermodynamics – A Contemporary Perspective (New Physics Series)*, Baifukan, Co., LTD, pp.20-80, 2000.
[21] P. Wilmott, *Derivatives*, John Wiley & Sons, 1998.